

Electrospun zirconium hydroxide nanoparticle fabrics as sorptive/reactive media

Ryszard Wycisk · Dushyant Barpaga ·
Stephen Pintauro · M. Douglas LeVan ·
Peter N. Pintauro

Received: 4 June 2013 / Accepted: 20 September 2013 / Published online: 1 October 2013
© Springer Science+Business Media New York 2013

Abstract Good quality adsorbent fabrics were electrospun from slurries of zirconium hydroxide nanoparticles and polyvinyl butyral (PVB) in alcohols. The as-spun fabrics had very high porosity, about 80 vol%, and high zirconium hydroxide content, 50–95 wt%. The porosity and mechanical strength of the fabrics could be modified via compaction and/or exposure to alcohol vapor. SO₂ sorption capacity of the fabrics was high at 1.6–1.9 mol/kg and was relatively independent of the sample pretreatment, unlike the capacity of the pristine nanoparticles, which decreased when the powder was stored in a low relative humidity atmosphere. The as-purchased zirconium hydroxide nanoparticles contained about 45 wt% of water, equivalent to the formula ZrO₂·5.6H₂O. In contrast, the electrospun composite fabrics contained only 25 wt% of mostly coordinated water, leading to the formula ZrO₂·2.2H₂O. The presence of PVB binder inhibited the rehydration/dehydration processes and stabilized the SO₂ sorption capacity of the composite fibers. The electrospun fabrics could find applications as conformable, flexible filters in civilian and military applications.

Keywords Electrospinning · Zirconium hydroxide · Polyvinyl butyral · Sorbent · SO₂

1 Introduction

Electrospinning is a fabrication process that utilizes electrostatic charging of polymer solutions or melts for the formation of ultrafine fibers with diameters in the nanometer to micrometer range. Electrospun nanofibers have been shown to be effective in diverse applications ranging from air filtration (Grafe and Graham 2003), fuel cells (Choi et al. 2010; Zhi et al. 2012), and solid-phase extraction (Chigome et al. 2011). Advantages of electrospun nanostructures are numerous and include high specific surface area, high interfiber volume fraction, controllable fiber diameter, wide range of polymers that can be employed, and availability of various post-processing methodologies. Additionally, the standard electrospinning setup is simple, consisting of a pump, spinneret, a high voltage power supply, and a fiber collector. Modern, high-throughput needleless electrospinning systems have been introduced recently by Elmarco (Laudenslager and Sigmund 2011).

While electrospinning of polymers and polymer composites, including adsorbents, with low content of solid particles has been well documented (Huang et al. 2003; Ostermann et al. 2011), fabrication of electrospun composites with high inorganic nanoparticle content is still in the early stages of developmental maturity. These hybrids differ from the classical electrospun sol–gel systems (Ma et al. 2011) in that the polymer carrier/binder is retained and not removed during the high-temperature calcination process.

An example of such a highly scalable, electrospinning methodology has recently been disclosed by Zhang and Pintauro (2011). There, the hybrid nanofibers are electrospun from suspensions of solid nanoparticles containing small amounts of a suitable polymeric carrier/binder. The

R. Wycisk (✉) · D. Barpaga · S. Pintauro ·
M. D. LeVan · P. N. Pintauro
Department of Chemical and Biomolecular Engineering,
Vanderbilt University, Nashville, TN 37235, USA
e-mail: ryszard.wycisk@vanderbilt.edu

resultant fibers have diameters in the submicron to micron range and high particulate loadings. No high temperature firing or sintering is required, and the presence of polymer binders imparts mechanical robustness to the fibers. Additionally, various morphologies can be achieved, including uniform dispersion of nanoparticles and core-shell structures. These types of materials, containing carbon supported Pt, have been used as electrodes in hydrogen fuel cells where they outperform standard decal electrocatalysts (Brodt and Pintauro 2012).

Toxic gas removal is of great importance in a number of civilian and military applications. Efficient adsorbents designed for such applications should have appropriate porosities and specific chemistries ensuring high sorption capacities. For example, zirconium hydroxide, $\text{Zr}(\text{OH})_4$, has been shown recently to be an effective substrate capable of removing a wide range of reactive gases (Peterson et al. 2009).

In this paper, preliminary results on the fabrication and characterization of electrospun $\text{Zr}(\text{OH})_4$ nanoparticle-based fibrous sorbents are presented for the first time. The solid adsorbent content in the fabrics is high, up to 90 wt%, and the average fiber diameter is 400–1,000 nm.

2 Experimental

Zirconium hydroxide, also called hydrous zirconia, nanoparticles were purchased from US Research Nanomaterials, Inc. The average particle size was 40 nm and the specific surface area was 25–50 m²/g. Polyvinyl butyral (PVB, actually the copolymer poly(vinyl butyral-co-vinyl alcohol-co-vinyl acetate), $M_w = 170,000\text{--}250,000$), containing 80 % vinyl butyral units was purchased from Aldrich. Isopropanol (IPA) and butanol (BA) were also purchased from Aldrich.

Electrospinning slurries were prepared by mixing $\text{Zr}(\text{OH})_4$ powder with PVB in a IPA/BA (90 wt% IPA) solvent. A suspension of $\text{Zr}(\text{OH})_4$ was first sonicated for 90 min with intermittent mechanical stirring before the addition of PVB. The entire mixture was then stirred for approximately 20 h. The total polymer and $\text{Zr}(\text{OH})_4$ content of the spinning slurry was 10–65 wt%, and the $\text{Zr}(\text{OH})_4$ content was 2–60 wt%. The slurry was drawn into a 5 mL syringe and electrospun using a 22-gauge stainless steel needle spinneret, where the needle tip was polarized to a potential of 7–12 kV relative to a grounded stainless steel rotating drum collector. The spinneret-to-collector distance was fixed at 8 cm and the flow rate through the spinneret was held constant for all experiments at 1.25 mL/h. The electrospun fabrics were collected on aluminum foil attached to a cylindrical collector drum that rotated at 100 rpm. The drum also oscillated horizontally to improve the uniformity of deposited fabrics.

Electrospinning was performed at room temperature in a custom-built environmental chamber, where the relative humidity was maintained constant at 40 %. The thickness of the deposited fabrics was controlled by varying the duration of electrospinning. The fabrics were post-processed by mechanical compaction on a hydraulic press and/or exposure to methanol vapor which decreased porosity (increased fabric density).

Fabric porosity was estimated gravimetrically, by measuring weight and volume of the sample and dividing such obtained density by the effective density of the fiber calculated based on the composition and assuming density of PVB and $\text{Zr}(\text{OH})_4$ to be 1.08 and 3.25 g/cm³, respectively.

Thermogravimetric analysis was performed using a TA Instruments Q500 analyzer. Samples were heated in aluminum pans under 40 ml/min flow of nitrogen or air at a 10 °C/min ramp to 1,000 °C.

Equilibrium capacities for room temperature (23 °C) sulfur dioxide adsorption were measured using a breakthrough apparatus (Furtado et al. 2011). The concentration of SO_2 fed to the adsorbent bed was kept constant at 500 ppm. The capacity of the adsorbent, n (mol SO_2 /kg adsorbent), was calculated from

$$n = \frac{F}{m} \int_0^{\infty} (c_0 - c) dt \quad (1)$$

where c_0 is the feed concentration (mol/m³), and c is the effluent concentration at time t . F , the volumetric flow rate of SO_2 /air, was kept constant at 23 cm³/min. The mass, m , of the adsorbent was approximately 10–15 mg and was loosely packed in the column, which had an internal diameter of 5 mm.

Prior to breakthrough analysis, the adsorbent material was subject to three different pretreatment scenarios: (1) degassing under vacuum for 2 h at 70 °C, (2) equilibration in a stream of 50 % RH for 2 h, and (3) no special preconditioning with samples tested after being stored in the lab at 30–60 % RH.

3 Results and discussion

3.1 Electrospinning

Successful electrospinning of the $\text{Zr}(\text{OH})_4$ nanoparticles required finding an appropriate polymer carrier/binder and a suitable solvent. Based on the preliminary experiments, PVB was selected as the polymer carrier/binder, and a mixture of isopropanol/butanol was used as the solvent. A number of electrospinning slurries were prepared containing 5–60 wt% $\text{Zr}(\text{OH})_4$ and 2–10 wt% PVB. For every slurry composition, the electrospinning conditions were

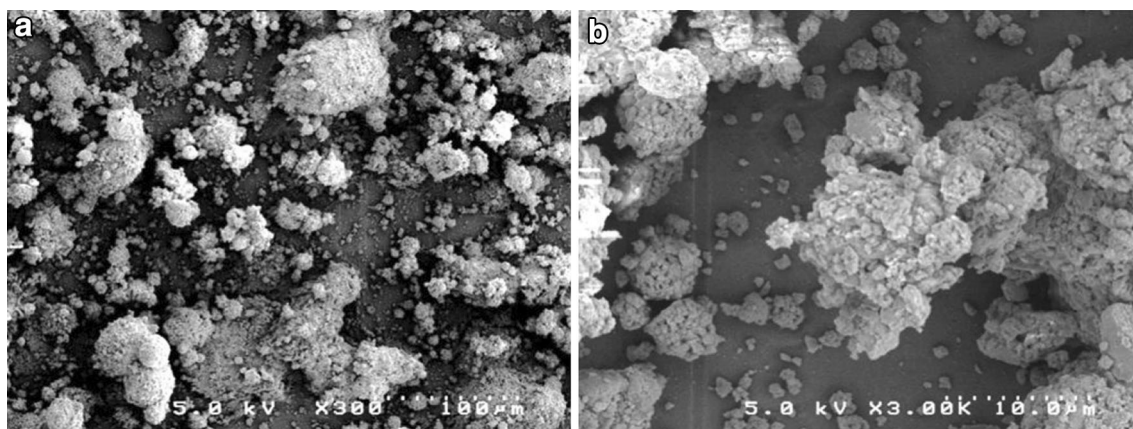


Fig. 1 SEM micrographs of electrospayed deposits obtained with improper electrospinning conditions (voltage too low, 4 kV). Magnification **a** 300 times and **b** 3,000 times

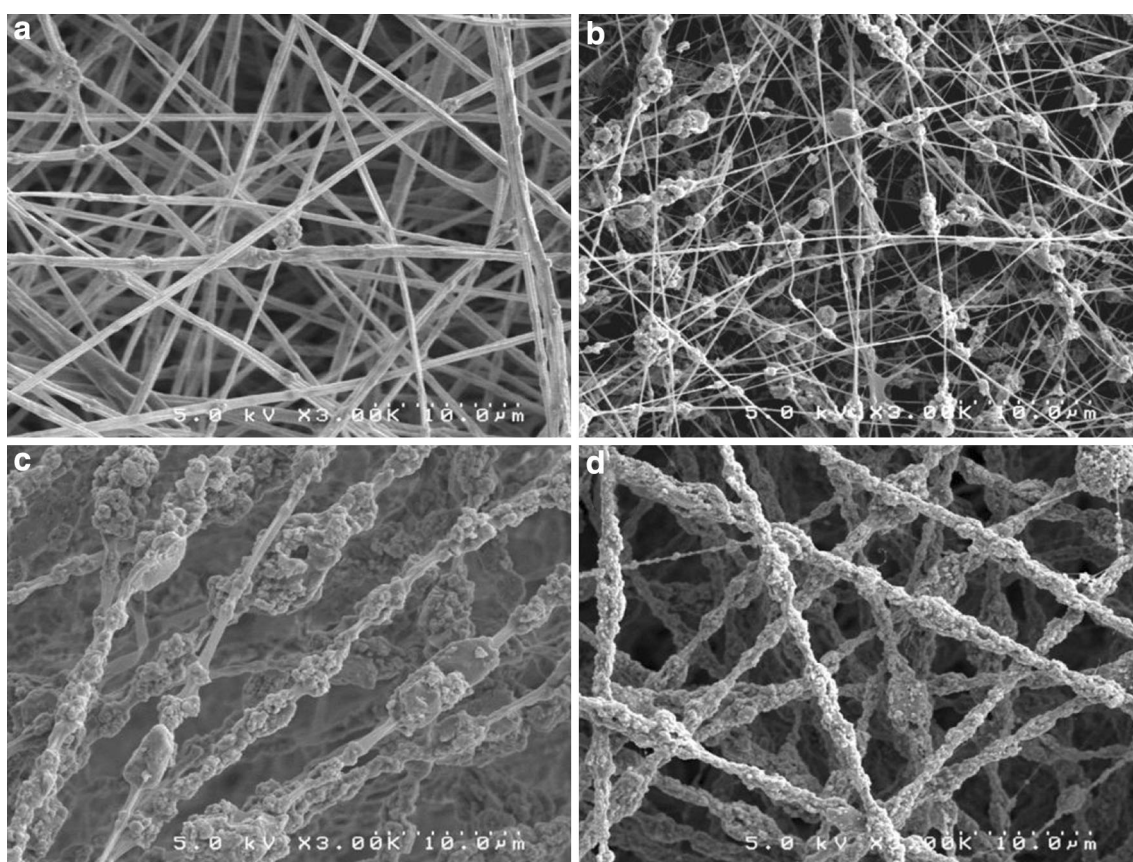
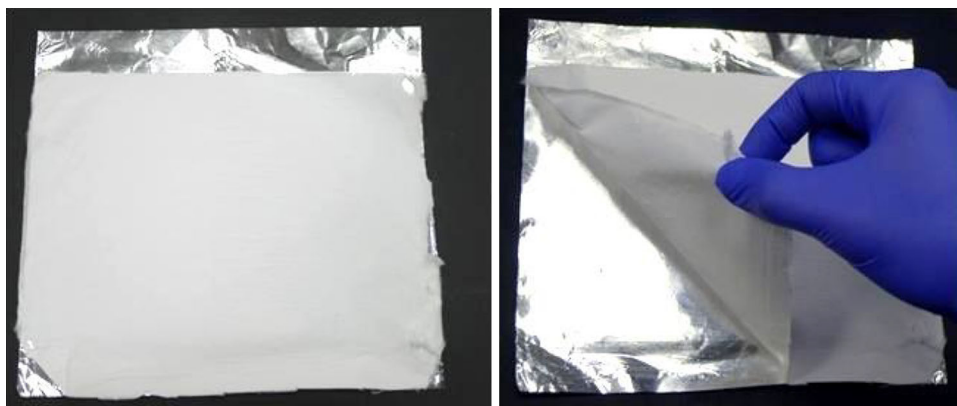


Fig. 2 SEM micrographs of the adsorbent fabrics electrospun from slurries with different Zr(OH)_4 -to-PVB weight ratios: **a** 1:2, **b** 2:1, **c** 5:1, and **d** 10:1. Magnification is 3,000 times

individually optimized to obtain fibers. When electrospinning conditions were not right the slurry was electrospayed and no fibers were obtained (Fig. 1). Many initial electrospinning attempts failed to give fabrics with uniform nanoparticle distribution due to the Zr(OH)_4 content in the slurry being very low, less than 10 wt%, which was somewhat surprising. In Fig. 2a–d, selected scanning

electron microscopy (SEM) images are shown to indicate the morphology of the composite fibers electrospun from slurries of different compositions. When the nanoparticles-to-polymer weight ratio was low (1:2), and the slurry concentration was 10 wt%, the fibers were nearly all PVB with a small amount of zirconium hydroxide agglomerates (Fig. 2a). At a higher weight ratio (2:1), more and bigger

Fig. 3 Photographs of the electrospun $\text{Zr}(\text{OH})_4$ -PVB fabric removed with the aluminum foil support from the collector drum (*left*) and partially peeled-off from the foil (*right*). Electrospinning conditions: 50 wt% $\text{Zr}(\text{OH})_4$ and 5 wt% PVB in the slurry, flow rate 1.25 mL/h, 10 kV, 8 cm spinneret-to-collector distance, 40 % RH



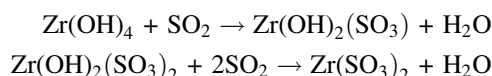
agglomerates were observed (Fig. 2b). When the relative content of $\text{Zr}(\text{OH})_4$ with respect to PVB was increased further (5:1), and the slurry concentration was raised to 35 wt%, the fraction of “naked fibers” was reduced dramatically (Fig. 2c). When the slurry contained 40 wt% $\text{Zr}(\text{OH})_4$ and 4 wt% PVB, good quality fabrics were electrospun with relatively uniform distribution of the nanoparticles in the fibers; the $\text{Zr}(\text{OH})_4$ content in the fibers was 85 wt%, lower than the expected 91 wt% due to a partial dehydration of the nanoparticles during the electrospinning (Fig. 2d).

In general, good mats were obtained from slurries containing a high $\text{Zr}(\text{OH})_4$ concentration and a low PVB binder concentration.

The electrospun fabrics were highly porous (80–85 vol%) but could be easily compacted to the desired porosity and additionally, the intersecting fibers could be welded to one another through exposure to alcohol vapors, which led to a dramatic increase of the mechanical strength. In Fig. 3 two photographs of an electrospun $\text{Zr}(\text{OH})_4$ -PVB fabric are presented. The thickness of the as-spun fabric, in general between 50–300 μm , was dependent on the amount of the slurry deposited. Even the unmodified fabric had strength sufficient to peel it from the aluminum foil support and to handle it without permanent deformation.

3.2 SO_2 adsorption testing

The mechanism of SO_2 adsorption on zirconium hydroxide has been studied by Peterson et al. (2009). Temperature-programmed desorption results indicated that SO_2 was strongly retained by the surface hydroxyl groups of $\text{Zr}(\text{OH})_4$. X-ray photoelectron spectroscopy results revealed the presence of sulfite (SO_3^{2-}) species following exposure, which suggested the formation of zirconium sulfite. The researchers proposed the following two-step reaction:



but concluded that the hydroxyl utilization was low, on the order of 10 %. Therefore, use of high surface area nanoparticle composite fabrics was envisioned to help improve the sorption capacity of $\text{Zr}(\text{OH})_4$.

Capacities of the electrospun fabrics were evaluated using a standard breakthrough setup with an in-line mass spectrometer for the feed of 500 ppm SO_2 in air at 23 °C. As expected, relatively high mat adsorption capacities were observed with the electrospun nanoparticle composites. For example, SO_2 capacities of 1.6–1.9 mol/kg were obtained with an electrospun $\text{Zr}(\text{OH})_4$ -PVB fabrics containing 50–95 wt% nanoparticles and an average fiber diameter of about 1 μm . That capacity was higher than that measured with silica derivatives and reported in the literature (Seredych and Bandosz 2010). Two sets of example breakthrough curves are shown in Fig. 4a, b.

Fast breakthrough was generally observed due to either very low nanoparticle bed height or very high bed porosity in case of the fabrics. Additionally, the curvature of the breakthrough curves differed between the two cases: it was convex for the pristine nanoparticles and concave for the electrospun fabrics, which is likely related to the dramatic differences in both, the bed characteristics and mass transfer properties.

The most important observation concerned the influence of the sample pretreatment on the measured capacity. It is evident that dehydration during degassing at 70 °C reduced the SO_2 sorption capacity of the nanoparticles by nearly 50 % compared to the sample equilibrated at 50 %RH, while practically no change was observed for the electrospun fabric. It can be concluded that dehydration during degassing affected the nanoparticle sorbent to a greater extent, compared to the electrospun composite fabric, and the adsorption capacity of the former was lowered. It is possible that the PVB binder stabilized the nanoparticles, thus improving the capacity retention in the fabrics.

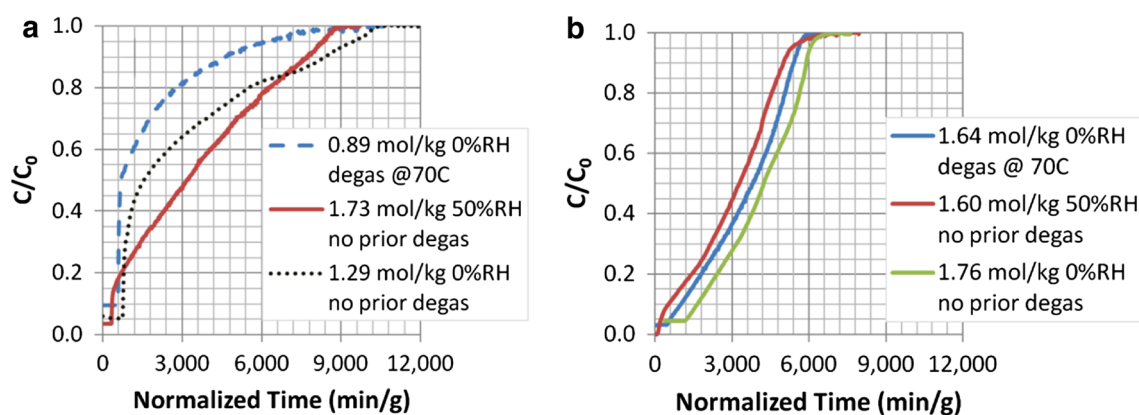


Fig. 4 SO_2 breakthrough curves recorded for **a** loosely packed bed of pristine $\text{Zr}(\text{OH})_4$ nanoparticles and **b** for a $\text{Zr}(\text{OH})_4$ -PVB composite fabric containing 10 wt% PVB. Different line types represent various sample pretreatments

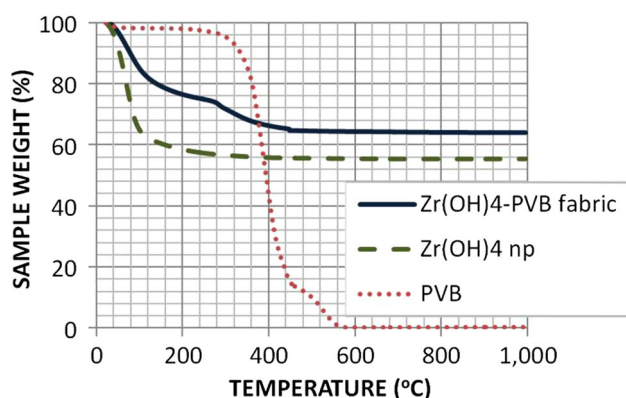


Fig. 5 Comparison of the three thermograms recorded, under nitrogen, for $\text{Zr}(\text{OH})_4$ fabric (solid line), $\text{Zr}(\text{OH})_4$ nanoparticles (broken line), and the PVB binder (dotted line)

3.3 Thermogravimetric analysis

Nano-zirconium hydroxide is an amorphous solid, insoluble in water, which decomposes at elevated temperature into zirconium oxide and water. An important complication associated with the use of zirconium hydroxide is that its water content is variable and its chemical formula is indeterminate, often described as $\text{ZrO}_2 \cdot n\text{H}_2\text{O}$. The dihydrate form with the formula $\text{ZrO}_2 \cdot 2\text{H}_2\text{O}$ is usually written $\text{Zr}(\text{OH})_4$ giving rise to its description as a hydroxide. It should be noted that totally dehydrated zirconium hydroxide would have practically no SO_2 sorption capacity, which was confirmed by testing the breakthrough curves of ZrO_2 nanoparticles giving the value of 0.04 mol/kg, negligibly small compared to that of $\text{Zr}(\text{OH})_4$ nanoparticles (0.89–1.73 mol/kg).

Thermogravimetry was used to determine the levels of hydration of the as-received nanoparticles and of the electrospun composite fabrics. A summary of the results is presented in Fig. 5. The dehydration process started at room temperature and concluded around 350–400 °C.

Most of the water was lost between 40 and 100 °C. PVB was stable to about 200 °C and disappeared completely at 560 °C.

It can be noticed that the as-purchased zirconium hydroxide nanoparticles contained about 45 wt% of water, corresponding to $\text{ZrO}_2 \cdot 5.6\text{H}_2\text{O}$. A significantly different result was obtained for the electrospun composite fabric. Taking into account the presence of PVB, the measured weight loss associated with the dehydration was only 25 wt%, leading to the formula $\text{ZrO}_2 \cdot 2.2\text{H}_2\text{O}$, and giving water content very close to the coordinated water limit. This indicates that most of the excess water was lost during the electrospinning and that the rehydration/further dehydration was inhibited, most probably, by the presence of the PVB binder.

4 Conclusions

Highly porous fabrics were electrospun from slurries of zirconium hydroxide nanoparticles and PVB binder in alcohols. Fiber diameter was in the 400–1,000 nm range. When the electrospinning slurry contained 40 wt% $\text{Zr}(\text{OH})_4$ and 4 wt% PVB, good quality fabrics were obtained with relatively uniform distribution of the nanoparticles in the fibers. The fabrics had reasonable strength and could be handled unsupported without permanent deformation. The SO_2 sorption capacity of the fabrics was high at 1.6–1.9 mol/kg and was relatively independent of the pretreatment, unlike the capacity of the pristine nanoparticles, for which the capacity decreased dramatically when the powder was kept at low relative humidity. The presence of the PVB binder inhibited the rehydration/dehydration processes and stabilized the SO_2 sorption capacity of the composite fibers. The electrospun composite fabrics could be used as conformable filters and sorbents for toxic gases removal.

References

- Brodt, M., Pintauro, P.N.: Low Pt-loaded nanofiber electrodes for hydrogen/air fuel cells, Abstract #1263. In: Pacific Rim Meeting on Electrochemical and Solid-State Science, Honolulu, October 2012
- Chigome, S., Darko, G., Torto, N.: Electrospun nanofibers as sorbent material for solid phase extraction. *Analyst*. **136**(14), 2879–2889 (2011)
- Choi, J., Zhang, W., Wycisk, R., Pintauro, P.N., Lee, K.M., Mather, P.T.: High conductivity perfluorosulfonic acid nanofiber composite fuel cell membranes. *ChemSusChem*. **3**, 1245–1248 (2010)
- Furtado, A.M.B., Liu, J., Wang, Y., LeVan, M.D.: Mesoporous silica-metal organic composite: synthesis, characterization, and ammonia adsorption. *J. Mater. Chem.* **21**, 6698–6706 (2011)
- Grafe, T.H., Graham, K.M.: Nanofiberwebs from electro-spinning. In: Proceedings of the 5th International Conference on Nonwovens in Filtration, Stuttgart, 1–5 (2003)
- Huang, Z.-M., Zhang, Y.-Z., Kotaki, M., Ramakrishna, S.: A review on polymer nanofibers by electrospinning and their applications in nanocomposites. *Compos. Sci. Technol.* **63**, 2223–2253 (2003)
- Laudenslager, M.J., Sigmund, W.M.: Developments in electrohydrodynamic forming: fabricating nanomaterials from charged liquids via electrospinning and electrospraying. *Am. Ceram. Soc. Bull.* **90**(2), 2–26 (2011)
- Ma, Z., Huijiao Ji, H., Teng, Y., Dong, G., Zhou, J., Tan, D., Qiu, J.: Engineering and optimization of nano- and mesoporous silica fibers using sol-gel and electrospinning techniques for sorption of heavy metal ions. *J. Colloid Interface Sci.* **358**, 547–553 (2011)
- Ostermann, R., Cravillon, J., Weidmann, C., Wiebcke, M., Smarsly, B.M.: Metal-organic framework nanofibers via electrospinning. *Chem. Commun.* **47**, 442–444 (2011)
- Peterson, G.W., Karwacki, C.J., Feaver, W.B., Rossin, J.A.: Zirconium hydroxide as a reactive substrate for the removal of sulfur dioxide. *Ind. Eng. Chem. Res.* **48**(4), 1694–1698 (2009)
- Seredych, M., Bandoz, T.J.: Effects of surface features on adsorption of SO₂ on graphite oxide/Zr(OH)₄ composites. *J. Phys. Chem. C* **114**, 14552–14560 (2010)
- Zhang, W., Pintauro, P.N.: High-performance nanofiber fuel cell electrodes. *ChemSusChem*. **4**, 1753–1757 (2011)
- Zhi, M., Lee, S., Miller, N., Menzler, N.H., Wu, N.: An intermediate-temperature solid oxide fuel cell with electrospun nanofiber cathode. *Energy Environ. Sci.* **5**, 7066–7071 (2012)